Part IV
Emerging Technologies

17 Patch-Clamp Technologies for Ion Channel Research

Fred J. Sigworth and Kathryn G. Klemic

The electrical activity of living cells can be monitored in various ways, but for the study of ion channels and the drugs that affect them, the patch-clamp techniques are the most sensitive. In this chapter the principles of patch-clamp recording are reviewed, and recent developments in microfabricated patch-clamp electrodes are described.Technical challenges and prospects for the future are discussed.

17.1 Introduction

The human genome contains more than 400 genes that code for ion channels. How are all of these channel types to be characterized? The standard tests of a new channel type—its ion selectivity, conductance, voltage dependence, ligand sensitivity—traditionally require weeks of effort by a PhD-level scientist. Then, besides the basic characterization, are questions about accessory proteins or posttranslational protein modifications that may alter an ion channel's behavior in significant ways. The functional understanding of each ion channel type presents a difficult but important problem.

Ion channels are also contributors to various diseases (Kass, 2005), and they are important targets for drugs. The large number of distinct ion channel types is an advantage for therapeutics, because it means that a drug targeted to a particular ion channel type that is expressed in one tissue is less likely to have undesired side effects in another tissue. Thus for example an immunosuppressive drug targeted to the potassium channels of lymphocytes will not affect the different potassium channels found in the nervous system (Vennekamp et al., 2004). The screening of compounds to find specific ion-channel blockers or modulators is therefore of great interest.

The understanding of biophysical transduction mechanisms of ion channels is also important. How do changes in membrane potential, or mechanical stretch, or the concentration of transmitter molecules, result in the activation of ion channels? Studies of these mechanisms, and ways to modulate them are discussed in other chapters of this volume. Progress in these areas would be aided by more sensitive and higher-throughput methods for recording ion channel currents.

Fred J. Sigworth and Kathryn G. Klemic

In mechanism and, in some cases, in structure, ion transporters are related to ion channels. These "pumps" and "carriers" are studied with some of the same tools as ion channels, including voltage-clamp and patch-clamp measurements of electrical current. However, the current produced by the operation of an ion transporter is orders of magnitude smaller than that of an ion channel. There are substantial technical challenges in being able to record these small currents.

17.1.1 The Need for High Throughput

The functional analysis of ion-channel genes and the screening of pharmaceutical compounds that affect particular ion channels require much higher-throughput assays of ion channel activity than the traditional patch-clamp technique. Emerging chip-based technologies, especially planar patch-clamp technology, are beginning to make large-scale screens of genes and compounds possible.

An illustrative example of the need for higher-throughput evaluation of channel behavior is the problem of drug-induced cardiac arrhythmias. Some people are susceptible to the acquired long-QT syndrome (Roden, 2004) arising from the drug-induced blockade of the hERG potassium channel (Fig. 17.1). The Q-T interval of the electrocardiogram is a measure of the duration of the action potentials in the ventricles of the heart. If the Q-T interval of one action potential is too long, the ventricular muscle will not be able to respond uniformly to the subsequent beat, and the desynchronization of the ventricular cells results in chaotic electrical activity and sudden death.

Several common drugs have been taken off the market, or their use curtailed, because they have caused sudden death due to cardiac arrhythmias (Brown, 2004;

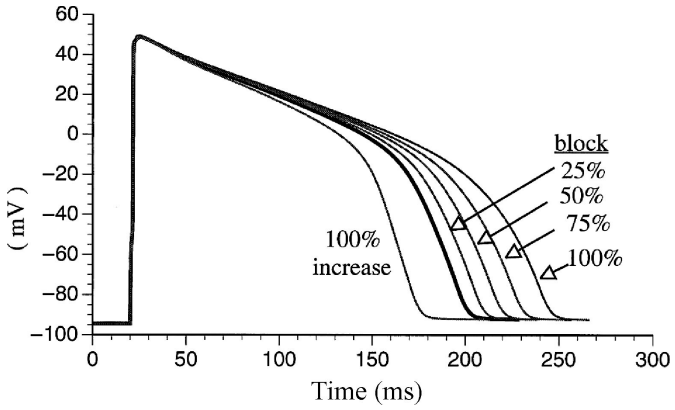

Fig. 17.1 Simulated action potentials in a ventricular muscle cell of the heart, from Zeng et al. (1995). Blocking the I_{Kr} current carried by hERG channels produces a lengthening of the action potential. The duration of the ventricular action potential is reflected in the Q-T interval of the electrocardiogram.

Roden, 2004). The U.S. Federal Drug Administration now requires that every drug be screened for an effect on the Q-T interval, and recommends a test for drug effects on hERG channel function.

17.1.2 The Need for Higher Sensitivity

The best-studied ion channels have conductances of 100 pS or more. With driving forces of 100 mV, these channels carry currents of more than 10 pA, which is easily recorded with the conventional patch-clamp technique, which yields measurements with an rms noise level of about 0.1 pA with a 1 kHz recording bandwidth.

There are however very important channels that carry smaller currents—the voltage-gated calcium channels of neurons and the chloride channels whose dysfunction causes Cystic Fibrosis, to name two. The currents carried by these channels are on the order of 0.1 pA, fewer than 10^6 elementary charges per second. Much smaller currents, about $100e_0$/s, are carried by ATP-driven ion pumps and other ion transporters. The grand challenge would be to resolve the displacement of a single elementary charge across the membrane. With such resolution, the individual movements of the voltage sensors in a potassium or sodium channel could be monitored, and the sequence of displacements in the transport cycle of an ion pump or transporter protein would be open to inspection.

As we shall see in Section 17.5, there are two major determinants of the noise level of a patch-clamp system. One is the thermal noise in the seal resistance and the electrode dielectric. The second is a noisy current that arises from the voltage noise in the amplifier as it is imposed on the capacitance of the input circuit, including the electrode itself. The controlled geometry of chip electrodes can be exploited to especially reduce the second noise source, so that their low capacitance, combined with high-performance amplifier devices, may allow single-elementary-charge resolution to be approached.

17.2 Recordings of Ion Channel Activity

17.2.1 Measurement of Membrane Potential

The activity of ion channels is reflected in a cell's membrane potential. The membrane potential is defined to be the voltage difference from the inside to the outside of the cell's bounding membrane. The membrane potential is conventionally measured directly using a microelectrode, which is a saline-filled glass micropipette that impales the cell. Alternatively, the membrane potential can be monitored (with somewhat less precision) using voltage-sensitive optical probes.

An electrical model for a cell membrane (Fig. 17.2) is a capacitance in parallel with various current sources that represent the ion channel currents. The membrane

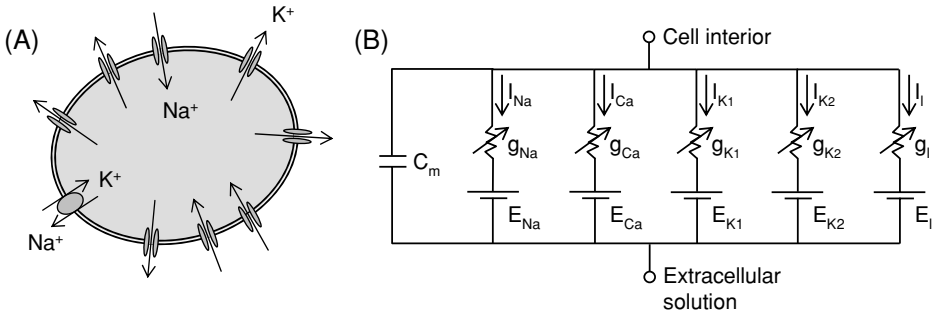

Fig. 17.2 Models for electrical activity in a cell. (A) About 15 μm in diameter, a "typical" mammalian cell contains hundreds of ion channels of several different types in its plasma membrane, as well as many copies of transport proteins including the ATP-driven sodium–potassium pump diagrammed here. (B) Electrical model of the cell. The membrane presents a capacitance of about 10 fF/μm^2 of surface area, roughly 20 pF for a mammalian cell. The total current from a population of ion channels is represented by a conductance, that varies according to the fraction of channels open, in series with a battery representing the reversal potential of the channel type. At rest the total conductance may be 1 nS, but at the peak of an action potential the conductance can be 1000 times larger. The reversal potentials are generally nonzero because of differences in ion concentration across the membrane.

potential E depends on the ion channel currents I_j according to

$$C_{\mathrm{m}}\frac{dE}{dt} + \sum_j I_j = 0. \tag{17.1}$$

The current carried by the jth ion channel type is then modeled with a conductance g_j,

$$I_j = g_j(E - E_j), \tag{17.2}$$

where g_j itself is typically a function of both E and time. The reversal potential E_j represents the electrochemical driving force on the ions that pass through the channels. For example, for potassium channels $E_{\mathrm{K}} \approx$ –90 mV while the reversal potentials E_{Na} for sodium, and E_{Ca} for calcium channels typically are about +60 mV. At rest, nerve and muscle cells have a membrane potential in the range of –70 to –90 mV that reflects a preponderance of potassium conductance. Action potentials occur when large sodium or calcium conductances drive the membrane potential transiently to values of +50 mV or so.

Au: This sentence seems contradictory. You say there is a change in membrane potential that may have a small effect on the membrane potential.

The fact that multiple channel types contribute to the membrane potential makes it a poor reporter of ion channel activity in some cases. A cell typically has several potassium channel types in its membrane, all of which contribute to the resting potential. The change in membrane potential due to the activation or block of one of these channel types can have a very small effect on the membrane potential due to the parallel conductance of other channel types.

Voltage-gated sodium channels, on the other hand, are responsible for the fast action potentials in neurons and muscle cells, including cardiac muscle. The presence of action potentials in these cells, and their "fatigue" with repetitive stimulation, is strongly dependent on the properties of the sodium channels. Methods for recording membrane potentials with high time resolution can therefore provide useful information, for example, about use-dependent block of sodium channels. New, highly sensitive optical probes of membrane potential are approaching the required time resolution (Gonzalez and Tsien, 1997).

17.2.2 Extracellular Measurements

In some cases action potentials can be detected with electrodes placed outside a cell. The signals are very small, typically less than 1 mV in amplitude, and result from voltage drops in the bathing solution due to extracellular current flow. The amplitude of these signals is highly variable, and depends on the exact geometry of the cell and the extracellular current pathways. Thus as an assay of channel activity extracellular measurements contain less information than membrane potential measurements. Extracellular microelectrode arrays are nevertheless useful in monitoring the action potential activity from a population of cells, for example, in small networks of neurons, in brain slices, and in heart tissue.

Might it be possible to measure directly the membrane potential with an extracellular device? The cell membrane is a self-assembled bilayer of lipid molecules, containing a hydrophobic core about 5 nm thick. The membrane potential produces a large electric field within the membrane core, which might be coupled directly to a field-effect semiconductor device. This approach has been pursued by two groups (Hutzler and Fromherz, 2004; Ingebrandt et al., 2005) (Fig. 17.3). Unfortunately, a layer of ionic solution is interposed between the cell and the device, whose thickness is large compared to the Debye length (about 1 nm) of the solution; thus the electric field at the device surface greatly attenuated. Indeed, the small signals amplified by

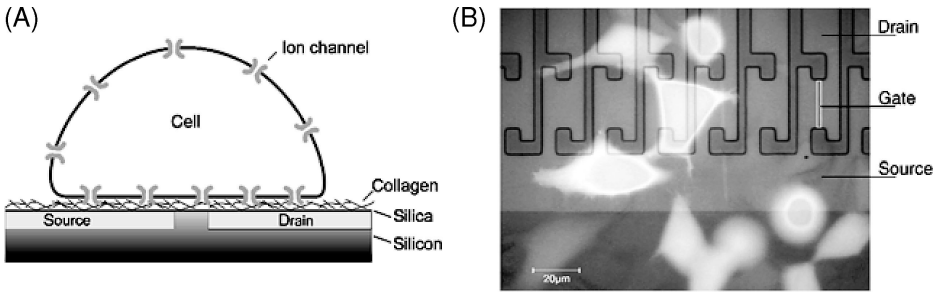

Fig. 17.3 Cell–FET interface. An open-gate field-effect transistor (A) senses the potential in the vicinity of the cell membrane. (B) A photograph of cells on an FET array. From Fromherz (2002).

these field-effect transistors arise mainly from extracellular current flow rather than the direct field effect (Braun and Fromherz, 2004).

17.2.3 Measurements of Ion Flux

Another way to monitor ion channel activity is by measuring the transport of ions across the cell membrane. The activity of ion channels generally produce only small and slow changes in ion concentration in a cell, making this measurement difficult for most ion channel types. There are however two notable exceptions. In the case of most potassium channels, rubidium ions can serve as an excellent tracer, and fluorescent dyes sensitive to rubidium report the total permeability of the channels (Terstappen, 1999).

The situation is even better for calcium channels, because local Ca^{2+} fluxes can be measured with very high sensitivity. The cytoplasmic free calcium concentration is very low, roughly 100 nM, maintained by buffering and active pumping. Meanwhile high-affinity Ca^{2+}-sensitive fluorescent dyes can readily detect micromolar Ca^{2+} concentration changes. The result is the ability to detect the local calcium "sparks" accompanying the opening of single Ca^{2+}-permeable channels. This has been extremely useful in studying the activity of the channels that release calcium from intracellular stores (Cheng et al., 1993; Baylor, 2005), but has also been used to observe the opening and closing of single neurotransmitter-receptor channels (Demuro and Parker, 2005). The disadvantage is that sophisticated optical system (confocal or total internal reflection excitation) must be used to keep the background fluorescence low; however a very interesting feature of Ca^{2+}-imaging is that the activity of hundreds of individual channels can be recorded simultaneously, even with millisecond time resolution.

17.2.4 The Patch-Clamp Techniques

A direct electrical measurement of ion channel activity is provided by voltage-clamp techniques, in which an injected current I_{inj} is supplied to balance the ion channel currents (Fig. 17.4),

$$C_{\text{m}}\frac{dE}{dt} + \sum_j I_j = I_{\text{inj}}. \tag{17.3}$$

If E is held constant, the injected current becomes equal to the sum of the channel currents. I_{inj} is then recorded as a direct measure of the ion channel current. A voltage-clamp system (Fig. 17.4) uses an operational amplifier to set the potential while measuring the current, and requires a low value of the series resistance R_{s} to make a high-quality recording.

The patch-clamp methods were originally developed by Neher, Sakmann and colleagues (Neher et al., 1978) to observe the activity of single ion channels. The

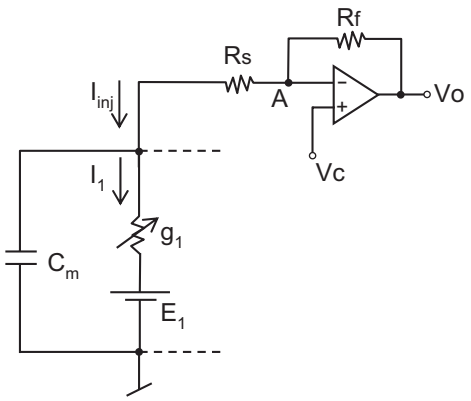

Fig. 17.4 Model of a cell and voltage-clamp system. The current I_{inj} is equal to the total ionic current through channels I_i provided the voltage across the membrane capacitance C_m remains constant. An operational amplifier forces node A to be at the potential V_C while also providing the current monitor output voltage $V_O = R_f I_{inj} + V_C$. Thus the injected current is measured while the membrane potential is held approximately at V_C. The series resistance R_s of the electrode however causes the actual membrane potential to be in error by the amount $R_s I_{inj}$, so it is important that the series resistance be kept relatively small.

idea was to electrically isolate a small area of cell membrane (containing only a few ion channels) and to minimize the thermal noise in the recording system. To establish a patch-clamp recording, the tip of the glass pipette is gently placed against the cell membrane (Fig. 17.5A). The pipette tip is visualized in a microscope and is moved by a micromanipulator controlled by a skilled operator. When sealed against the cell membrane, the pipette collects most of the current flowing through the patch of membrane, delivering it to a current-measuring amplifier (Fig. 17.5B). A high resistance pipette-membrane seal allows the background noise to be low. For example, a seal leakage resistance $R_L = 10$ GΩ yields a noise standard deviation (rms value) of 0.13 pA at 10 kHz bandwidth. A poor seal with resistance $R_L = 100$ MΩ produces ten times the noise, 1.3 pA rms.

The key feature of the modern patch-clamp technique is the tight glass-to-membrane seal (Hamill et al., 1981) whose mechanical stability means that the seal remains intact even if the membrane patch is ruptured (by suction or voltage pulses) or excised, in the latter case resulting in a cell-free membrane patch. Cell-free patches are ideal for studying the effects of solution changes on channel activity, as the solution bathing the pipette can be changed on a millisecond timescale without disturbing the patch membrane. Changing the solution inside the pipette is however more difficult, and is a challenge that is being met in microfabricated devices.

Rupturing the membrane patch produces the most-used variant of the patch-clamp technique, whole-cell recording (Fig. 17.5C). This provides access to the cell interior with a series resistance typically in the range of 3–10 MΩ. The result is the ability to measure membrane potentials and to perform voltage-clamp measurements. The series resistance is not always negligible, because an error voltage equal

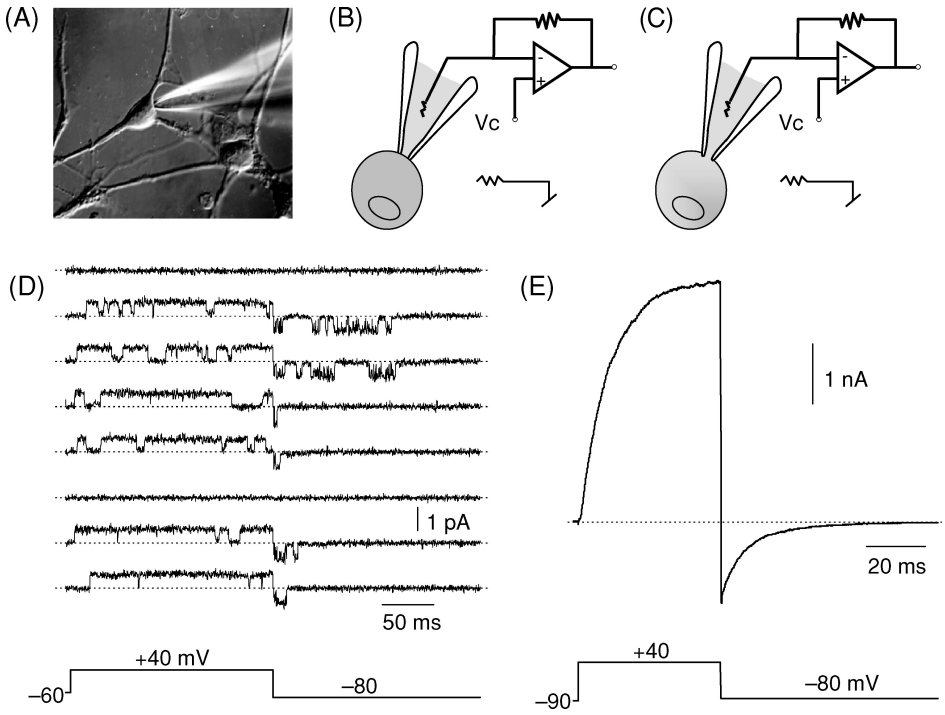

Fig. 17.5 Patch and whole-cell variants of the patch-clamp technique. (A) Photograph of a patch pipette sealed to a cultured neuron. (B) Schematic of an on-cell patch recording, where current is collected by the pipette from a small area of membrane. (C) Whole-cell recording, in which the patch membrane is ruptured, giving the pipette access to the cell interior. (D) Example recordings from a patch containing a single Kv2.1 voltage-gated channel, stimulated by the applied voltage waveform shown at the bottom. The reversal potential of this channel was about—30 mV, such that open channel currents are positive (outward) at +40 mV and negative (inward) at—80 mV. The successive sweeps were all obtained with the same voltage stimulus, demonstrating the stochastic behavior of single channels. (E) Whole-cell recording showing the current through a population of about 10^4 Kv2.1 channels. The depolarization to +40 mV elicits a gradual opening of channels; repolarization to—80 mV causes the channels to close on a time scale of about 20 ms. Leakage and capacitive currents have been subtracted from the recordings in (D) and (E), leaving only the ion channel currents.

to $R_s I_{inj}$ develops across it. For example, with currents of several nanoamperes the $R_s I_{inj}$ error is on the order of 10 mV, which can be a serious error in studying voltage-dependent channel activity. As Hodgkin et al. (1952) showed, these errors can be mitigated by using appropriate feedback, called series-resistance compensation. In the case of a patch-clamp recording, a voltage equal to $R_s I_{inj}$ is estimated and added to the pipette voltage, effectively canceling the series-resistance error (Sigworth, 1995).

The origin of the all-important tight glass-to-membrane seal is not entirely understood. What is known is that a very clean glass surface is required, and the

presence of divalent cations, particularly Ca^{2+}, helps in its formation. Under good conditions the measured seal resistance rises spontaneously, soon after the pipette touches the cell, as if the membrane is "zippering" up to the pipette surface. Otherwise, gentle suction applied to the back of the pipette can encourage sealing to occur. The seal, typically with a resistance greater than 1 gigaohm, is commonly called a "gigaseal."

17.3 Planar Patch-Clamp Technologies

The economic driving force for developing planar patch-clamp technologies has been the need for highly parallel, automated voltage-clamp recordings from cultured mammalian cells. A wide variety of approaches have been pursued, but in all of these devices the glass pipette is replaced with a micromachined, insulating partition that separates two chambers filled with saline. The partition contains an aperture, 1–2 μm in diameter that is the topological equivalent of the opening at the tip of a glass pipette. A cell seals against the partition such that a patch of its membrane covers the aperture. A pulse of pressure or voltage breaks the patch membrane, establishing the whole-cell recording configuration.

17.3.1 The Cell-Guidance Problem

The biggest technical challenge for automated patch-clamp recording has been the "precision guidance" problem, of providing a way for cells to be guided directly into contact with a recording site. Experience has shown that once a cell (or cellular debris) seals to the tip of a glass pipette or to a planar recording site, a residue remains that is very difficult to remove, and which prevents the subsequent formation of a gigaseal. Thus all patch-clamp devices use disposable chips, and systems are designed to make the first contact of a cell with the active site to be as successful as possible in forming a gigaseal.

As a microchip replacement for the glass pipette, a device made by Stett et al. (Stett et al., 2003; van Stiphout et al., 2005) is perhaps the most elegant (Fig. 17.6). Suction of fluid into the 10 μm outer channel guides a cell into contact with the inner (about 1 μm diameter) contact channel. The contact channel functions like the interior of a patch pipette; positive pressure is initially applied to prevent debris from approaching its surface, and then suction is applied to encourage seal formation when a cell is in place. This is the same procedure that is used with conventional pipettes.

A cross-section of this device (Fig. 17.6C and D) shows a complex profile that is created on a silicon wafer through many processing steps including the deposition and etching of SiO_2. The SiO_2 surface forms excellent gigaseals with cells, with a success rate for establishing seal resistances above 1 GΩ of about 90%. Cytocentrics CCS GmbH has announced a parallel, automated patch-clamp system

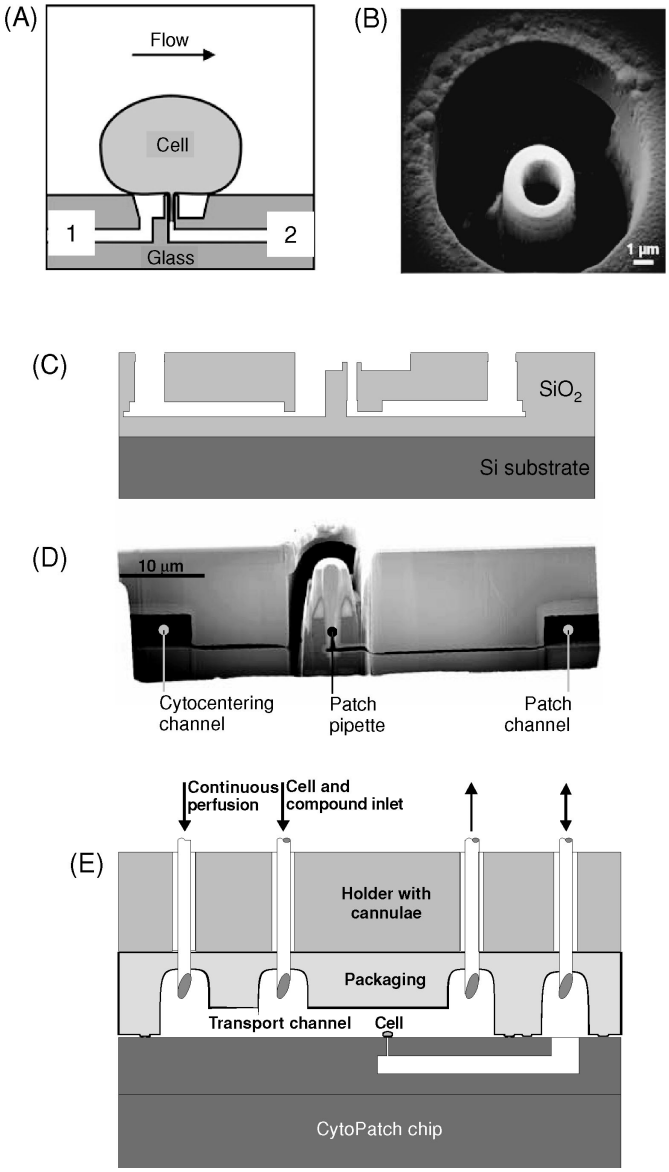

Fig. 17.6 The "cytocentering" chip. (A) Cross section. A cell is trapped by suction applied to the large port 1 of the device. Subsequent suction on the central port 2 forms a seal, and currents are recorded through port 2. (B) Scanning electron microscope (SEM) image of the device from above. (C) Cross section diagram of the device, showing the fluidic compartments. (D) Corresponding SEM cross-sectional view. (E) Cross section diagram of the packaged chip with fluidic ports. From van Stiphout et al. (2005).

using disposable chips based on this design. Another device that replaces the pipette tip with a micronozzle has been described by Lehnert et al. (2002).

Another technology for guiding cells toward apertures is dielectric focusing (Schmidt et al., 2000; Guia et al., 2002). A potential difference of several hundred millivolts is imposed across a silicon nitride membrane about 100 nm thick. The membrane has a micron-sized aperture, and the resulting electric field guides small nonconducting particles into the aperture. This system works well for liposomes, which are small artificial lipid-membrane structures. With an additional 20 nm SiO_2 layer on the membrane that is modified by an aminosilane or by adsorption of polylysine, gigaohm seals to liposomes were demonstrated. Unfortunately, for larger structures such as mammalian cells no success has been reported. We speculate that the larger electric fields required to manipulate cells would cause cell damage.

17.3.2 Loose Patch Clamp

A very different solution to the "precision guidance" problem is to not attempt the formation of gigaseals at all. The earliest patch-clamp recordings (Neher and Sakmann, 1976; Neher et al., 1978) were made under conditions where the seal resistance was only a few tens of megaohms; in this situation the pipette surface is separated from the cell membrane by an aqueous film on the order of 1 nm in thickness, and glass and membrane are held together by continuous suction. Similarly, in the planar patch-clamp system by Molecular Devices (Kiss et al., 2003) suction draws cells into contact with micron-sized holes in a polymer sheet. The resulting seal resistances are on the order of 100 MΩ. This yields substantial leakage currents which are however tolerable if the ionic currents to be measured are sufficiently large. Breaking through the patch membrane to allow whole-cell recordings is done with the pore-forming antibiotic Amphotericin B (Rae et al., 1991). The IonWorks HT instrument uses disposable, 384-well "PatchPlates" from which the instrument makes 48 recordings simultaneously.

Even with this simple system, cell-to-cell variability results in a success rate of only about 70% in practical screening for ion-channel effects of drugs. An astonishingly effective improvement on the original PatchPlate is the "Population Patch Clamp" system, also by Molecular Devices, Fig. 17.7. There the single aperture at the bottom of each well is replaced by an array of 64 apertures. If each aperture seals onto a cell, then the resulting parallel recording yields a sum of the current in the entire population of cells. But what if one or more apertures are left open? The low resistance of an open aperture produces a large leakage current. Surprisingly, in practice it is found that the leakage current is not excessively large (nearly all the apertures are plugged by something!) and the quality of the recordings is as good as a single-well recording, and much more reproducible. A success rate better than 95% is reported for wells yielding useful recordings (Handran et al., 2005).

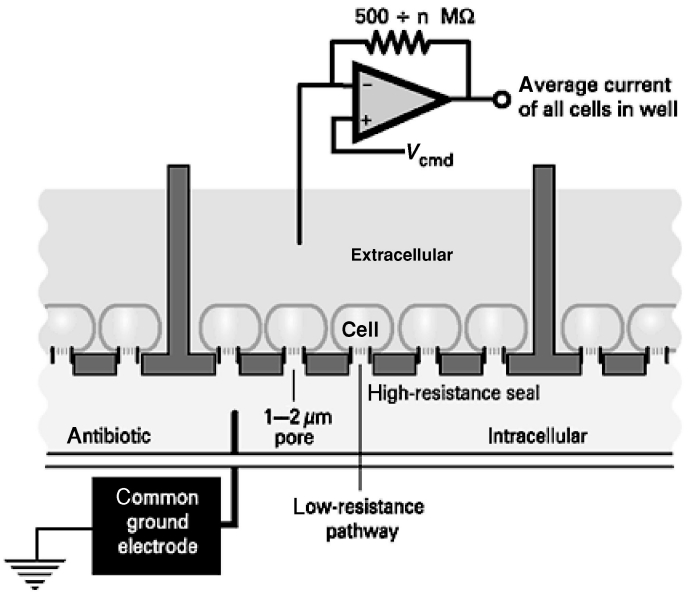

Fig. 17.7 Population patch-clamp device from Molecular Devices (Handran et al., 2005). At the bottom of a well are multiple apertures, against which cells are pressed by suction, and permeabilized by Amphotericin treatment. The current from the entire population of cells is monitored.

17.3.3 Planar Patch-Clamp Chips

Several groups have developed chips in which the cell seals against a planar surface having a simple round aperture. Lacking special fluidics, these systems rely on the use of a very dense and debris-free suspension of cells to provide a high likelihood of a cell coming to rest over the partition aperture (Fig. 17.8). Suction through the aperture helps in the final docking and sealing of the cell to the partition.

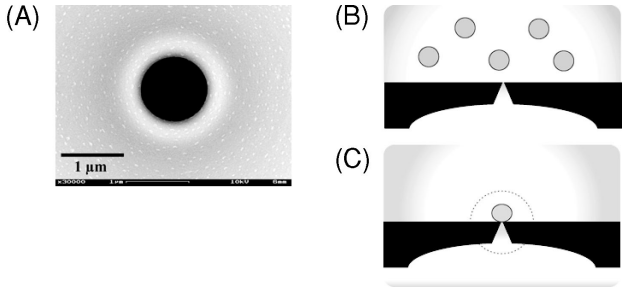

Fig. 17.8 A basic planar patch-clamp device made from glass or fused quartz. (A) Aperture in the planar "top" surface of a glass chip. (B) A cell suspension is applied to the top surface and suction is applied. (C) A cell seals over the aperture, allowing electrical recording. Unattached cells are washed away. Illustrations from Fertig et al. (2000, 2003).

The fabrication of a representative planar patch-clamp chip is diagrammed in Fig. 17.9. Here the partition is a self-supporting insulating membrane containing a micron-sized hole; it spans a window in a larger etched cavity in the bulk silicon substrate. Fig. 17.9A demonstrates how such a structure is made. The process starts with a silicon wafer having a thin layer of SiO_2 or Si_3N_4 grown or deposited on one surface. A micron-sized hole is etched in this layer to form the final aperture. Then an anisotropic etch of the back side of the wafer, forms the pyramidal cavity and leaves the suspended membrane. The first reported devices of this sort had a relatively thin, 120 nm Si_3N_4 membrane (Fertig et al., 2000). The formation of gigaseals in these devices was never observed, perhaps because the thin membranes provided insufficient sidewall area for forming the membrane seal. Such devices also show a large capacitance (hundreds of picofarads) across the partition, which would impair the noise performance even if gigaseals were formed.

Au: These films are grown or desposited. Oxide is either grown or deposited. Nitride is only deposited Ion implant is used to give a charged layer under the surface.

An improved device of this kind has been described by Sophion Bioscience (Asmild et al., 2003). After forming a suspended membrane, a thick layer of SiO_2 is deposited, forming a gently-rounded opening (Fig. 17.8C). The chips are employed in a 16-channel patch-clamp system, the Sophion QPatch. This system shows outstanding solution-exchange because of integrated microfluidics. After the silicon wafer is fabricated, a glass microfluidics wafer is bonded to it. The glass layer contains etched microfluidic channels which provide a pathway for the application of cells and also the rapid exchange of solutions. The bath solution chamber has a volume of 0.5 μl and can be exchanged completely in about 150 ms. This rapid exchange is very useful for the study of ligand-activated channels (Asmild et al., 2003)

In some devices the partition is made in silicon instead. The strategy is to form a micron-sized aperture in bulk silicon, and then grow silicon nitride and oxide layers to provide insulation. After a surface treatment these chips form gigaseals readily (Schmidt et al., 2000). Unfortunately, the quality of the recordings is limited by the large capacitance between the aqueous solutions and the bulk silicon, due to the relatively thin (<1 μm) insulating layer. In another silicon chip described by Pantoja et al. (2004) deep reactive-ion etching is used to define a micron-sized pore, onto which was deposited a SiO_2 layer. PDMS microfluidic layers are pressure-bonded to each side of the device, which allowed cell delivery and solution exchange while also reducing the electrical capacitance. Formation of gigaseals was rare, perhaps due to the roughness of the chip surface.

The most successful planar patch-clamp chips have been made of quartz or glass. The fabrication processes of commercial chips—in particular the way in which apertures are made—are proprietary. The only device of this kind whose exotic fabrication process has been described in detail (Fertig et al., 2002) is shown in Fig. 17.8A. A 200 μm fused-quartz wafer is thinned locally by wet etching to 20 μm thickness. The wafer is then penetrated by a single high-energy gold ion, which leaves a latent track that is selectively etched from one side. The etch yields a conical cavity that terminates in a micron-sized hole. These chips form gigaseals with cells and can be used for whole-cell and patch recordings (Fertig et al., 2002). Glass planar

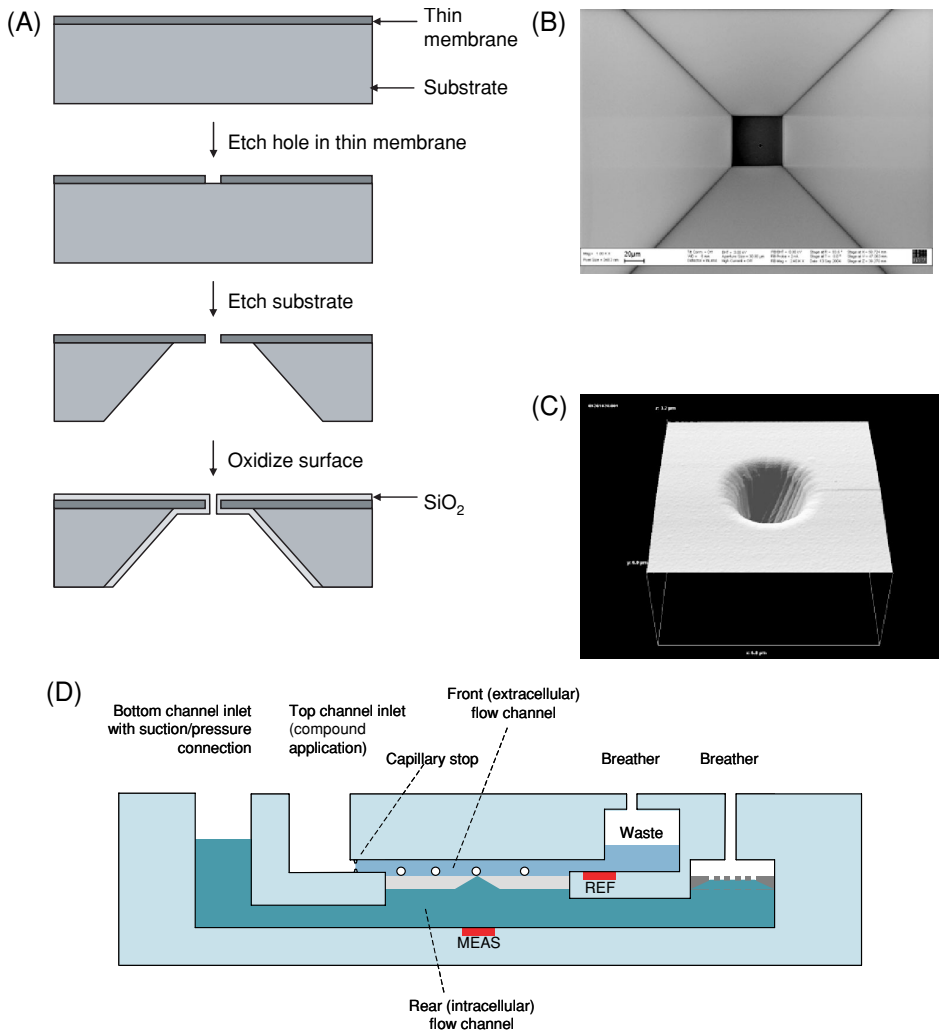

Fig. 17.9 An example of planar patch-clamp chip fabrication. (A) Process flow for fabricating a patch-clamp partition in a substrate with a thin membrane. The substrate is silicon with a thin silicon nitride or silicon oxide layer on top, only a few microns thick. The difference in composition permits preferential etching of either the substrate or the thin layer which will be used to form a membrane. (A) Micron-sized hole is etched in the membrane layer to form the final aperture. Then an anisotropic etch of the back side of the wafer, forms the pyramidal cavity and leaves the suspended membrane. (B) SEM view of the thin membrane of a finished device (Sophion QPatch chip), looking up through the pyramidal cavity in the substrate. A tiny dark spot marks the aperture. (C) AFM image of the top surface near the aperture, after deposition of an SiO_2 layer several microns thick. (D) The QPatch chip (center) is mounted in a carrier with microfluidic channels. Illustrations courtesy of Sophion Biosciences, www.sophion.com.

chips based on this general design are made by Nanion Technologies GmbH are used in single-well and 16-well recording systems (Fertig et al., 2003).

As a different sort of solution to the precision-targeting problem, Aviva Biosciences makes glass planar chips having a proprietary coating that greatly enhances the ability to form gigaseals. With this coating, simple suction through the aperture is sufficient to dock and seal a cell with a probability of about 75% (Xu et al., 2003). Chips from Aviva are used in the Molecular Devices PatchXpress instrument, which is a highly automated device that makes 16 simultaneous whole-cell recordings.

17.3.4 PDMS Patch Partitions

Polydimethylsiloxane (PDMS) is an elastomer that has many applications in microfluidics and biotechnology (Sia and Whitesides, 2003). Our laboratory has pursued the fabrication of simple patch-clamp partitions using micromolding of PDMS. The present fabrication method (Fig. 17.10) uses a stream of air to define a 2 μm hole in a PDMS sheet. Subsequent plasma oxidation of the cured PDMS forms a thin silica surface layer that is suitable for forming gigaseals with cells. Patch and whole-cell recordings can be made with the devices (Klemic et al., 2002, 2005). The probability of successful gigaseal recordings relatively low, presently about 25%; however, the fabrication method is easily scaled to form arrays of partitions, and is simple enough that it can be carried out in an electrophysiology laboratory.

Ionescu-Zanetti et al. (2005) have described a PDMS patch-clamp device in which the aperture is formed in the lateral wall of a microfluidic channel. This geometry allows very flexible transport of cells and solutions to the recording site. The formation of the lateral-wall aperture is challenging, and the success rate for forming gigaohm seals is low, about 5%, but in view of the easy integration with

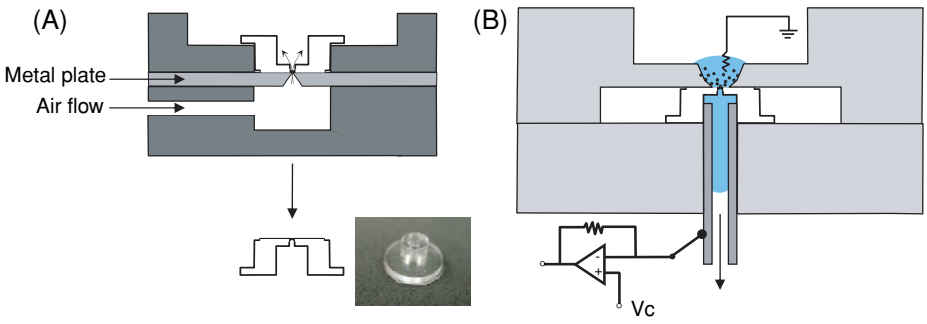

Fig. 17.10 PDMS planar patch-clamp device. (A) Fabrication. Air is forced through a 2 μm hole in a micromachined metal plate. A layer ~20 μm thick of PDMS resin is applied to the top of the plate and is surrounded by a pre-formed PDMS button. The plate is heated to cure the PDMS layer, the button is removed and treated in an oxygen plasma. (B) Cells are applied to the planar button surface. A chlorided silver tube inserted into the back of the button serves both as a suction port and electrode.

microfluidics this system is promising for situations in which a low-resistance seal is acceptable.

17.4 Simultaneous Electrical and Fluorescence Measurements

Fluorescent probes are an important tool in monitoring the molecular movements of proteins. The simultaneous recording of fluorescence changes and ion channel currents has been particularly useful in studying the movements of the voltage sensor of voltage-gated channels (Bezanilla, 2002). These measurements have been carried out on populations of channels, but particularly informative would be the ability to correlate spectroscopic changes of single reporter fluorophores with single channel currents. This has been done in one case (Borisenko et al., 2003) where fluorescently-labeled gramicidin A channels were detected in an artificial lipid membrane.

For channels in cell membranes, single-molecule fluorescence studies have been performed with cells under whole-cell voltage clamp (Sonnleitner et al., 2002). To avoid background fluorescence, the excitation light is provided by the evanescent wave, which illuminates a very thin ($\sim$100 nm) region above a glass surface. If a cell adheres to the surface, its membrane can be probed, but there is no room for a local patch electrode; hence whole-cell recording has been used up to now. It may be possible that the controlled geometry of planar patch-clamp devices might allow simultaneous electrical and optical recording from a small membrane patch with low fluorescence background.

17.5 The Grand Challenge: Single-Charge Detection

Starting in the 1970s patch-clamp recording provided the first biological "single molecule" measurements, as the open-closed conformational changes of single channels switched on and off picoampere-sized currents that could be recorded. Might it be possible to extend the sensitivity of membrane current recordings to be able to distinguish the movements of a few electronic charges?

With current patch-pipette technology the smallest detectable current pulse is on the order of 100 elementary charges. The sensitivity is limited by noise sources that have been analyzed in detail (Levis and Rae, 1998) and are summarized in Fig. 17.11. Current noise is most usefully described by the current spectral density $S_I(f)$ which has units of A^2/Hz. It is the variance in the measurement of current, making use of a narrow filter centered on the frequency f, and normalized by the bandwidth of the filter. The current spectral densities from independent sources are additive, so that the noise sources in a complete system consisting of patch membrane, electrode, and amplifier, can be separated into individual contributions. In an electrical model of the noise sources in a patch-clamp system (Fig. 17.11), the thermal noise in each

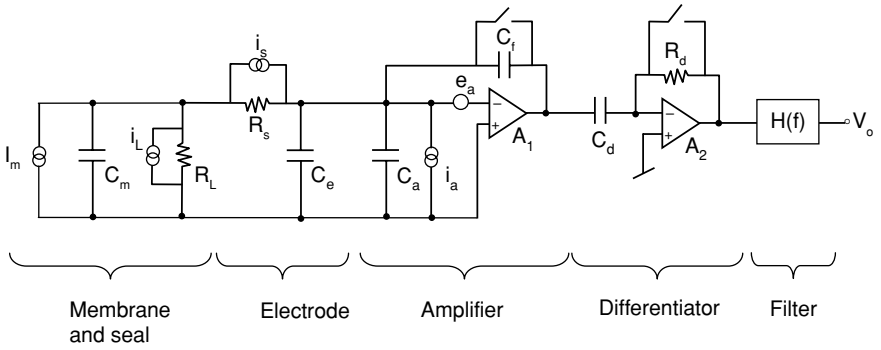

Fig. 17.11 Simplified equivalent circuit for a high-performance patch-clamp recording system using a capacitive-feedback amplifier for low noise. The output voltage is proportional to the patch membrane current I_m according to $V_o = R_d C_d I_m / C_f$ with filtering by a filter response $H(f)$. Switches allow periodic discharging of the integrating capacitor to allow DC currents to be recorded. Thermal noise sources in resistors (i_L, i_s) and amplifier input noise sources (i_a, e_a) are shown. Approximate component values for an optimized glass-pipette recording setup, along with values (in parentheses) for a hypothetical low noise planar electrode system are: patch membrane capacitance $C_m = 20(1)$ fF, seal resistance $R_L = 0.2(1)$ TΩ, electrode series resistance $R_s = 3(2)$ MΩ and electrode capacitance $C_e = 1(0.1)$ pF, amplifier input capacitance $C_a = 6(0.1)$ pF and amplifier noise $e_a = 2(0.5)$ nV/$\sqrt{\text{Hz}}$ and $I_a < 0.1$ fA/$\sqrt{\text{Hz}}$, $C_f = 1(0.1)$ pF. Another noise source is dielectric loss in the electrode capacitance, not modeled here.

actual resistance is modeled as a small random current generator in parallel with an idealized, noiseless resistance. The current generator for a resistance R has spectral density $4kT/R$, where k is Boltzmann's constant and T the absolute temperature. An amplifier is similarly modeled by an idealized amplifier with a noise voltage generator e_n and current generator i_n attached to its input.

The sum of all the noise sources in Fig. 17.11 yields an expression for the current spectral density having four terms,

$$S_I(f) = 4kT/R_L + i_a^2 + 16\pi^2 kTR_s C_m^2 f^2 + 4\pi^2 (C_m + C_e + C_a + C_f) e_n^2 f^2. \tag{17.4}$$

The first two terms give a frequency-independent spectral density (white noise). The first is the thermal noise in the seal leakage resistance R_L; with glass pipettes this resistance can be well over 10 GΩ and is comparable to the expected resistance of a few square microns of plasma membrane. The thermal noise current is $4kT/R_L$, which works out to about 1.6×10^{-30} A^2/Hz for $R_L = 10$ GΩ. Integrated over a bandwidth of 10 kHz this yields a variance of 1.6×10^{-26} A^2, or an rms noise of 0.13 pA. Smaller electrode apertures generally yield higher R_L values. The second term is the amplifier current noise spectral density i_a^2, which is expected to arise from shot noise in the gate leakage current (typically 1 pA or less) of the input transistor.

Au: You are missing a value here to end the sentence.

The third and fourth terms represent current spectral densities that increase steeply with frequency. The third comes from the thermal noise in the electrode series

resistance R_s as it is reflected in the patch membrane capacitance C_m. The fourth term is the reflection of the amplifier voltage noise in the total input capacitance. When all four terms are added together, the result is a spectral density that is constant at low frequencies but increases as f^2 at high frequencies. Fig. 17.12A shows the spectral density of the presently lowest-noise patch-clamp amplifier, the Molecular Devices AxoPatch 200B, measured with and without a low-noise fused-quartz pipette (Levis and Rae, 1998).

For practical purposes we would like to know the rms noise (i.e., the standard deviation of the noise) when the recording is filtered to a known extent, for example, by a Gaussian filter (Colquhoun and Sigworth, 1995) of a particular bandwidth. If the Gaussian filter's response is $H(f)$, then the rms current noise σ_I is obtained from the integral

$$\sigma_i^2 = \int_0^\infty S_i(f)\,|H(f)|^2\,df.$$

For the detection of very small charge movements, let us compare σ_I with the peak amplitude of the response to an impulse of current that represents a given number of elementary charges. Figure 17.12B shows the sensitivity of the recording system

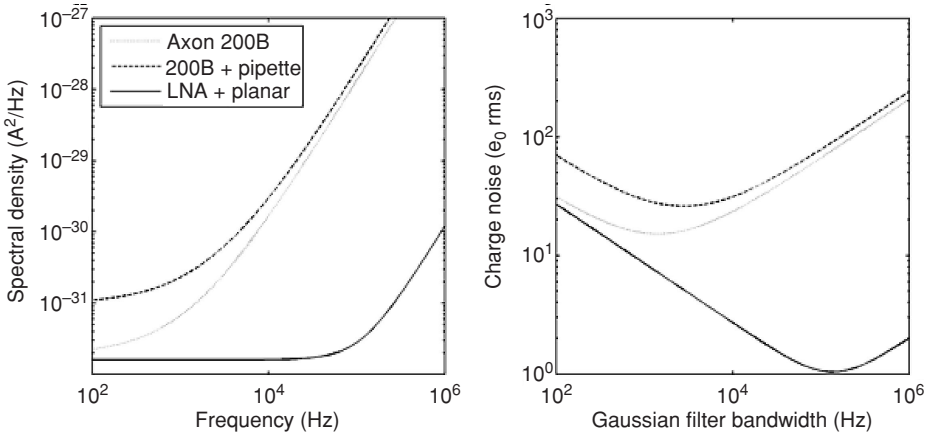

Fig. 17.12 Noise in patch-clamp recordings. A state-of-the-art amplifier (Axopatch 200B) alone and with an optimized fused-quartz pipette, is compared with a hypothetical low-noise amplifier and planar electrode. The left panel shows the input-referenced current spectral density as a function of frequency. The right panel is the equivalent rms charge noise as a function of filter bandwidth, computed as the ratio of rms current noise to the peak output of a Gaussian filter given an input of $1e_0 \times \delta(t)$. The pipette-based system has a charge noise of $25e_0$ rms at the optimum Gaussian filter bandwidth of 5 kHz. The hypothetical system (parameters given in the Fig. 17.9 legend) has a charge noise of $1e_0$ at a bandwidth of 200 kHz and would be able to detect individual charge pulses about $5e_0$ in magnitude.

evaluated in this way. What is plotted is the magnitude of a charge impulse whose expected peak value is equal to the standard deviation of the noise. This is plotted as a function of the bandwidth of a Gaussian low-pass filter. It can be seen that the present state-of-the-art amplifier and pipette combination yields a minimum charge noise of about 25 elementary charges rms.

Chip electrode technology makes improvements in electrode geometry that in principle can be exploited to make a very great decrease in noise levels. The legend of Fig. 17.11 gives parameters, and Fig. 17.12 gives noise performance, of a hypothetical electrode chip and amplifier that could reach a charge noise of $1e_0$ rms. How could this low noise level be reached? First, an electrode partition fabricated in quartz or PDMS could have a very small electrode solution volume and therefore decrease the electrode capacitance. A small aperture but a large solid-angle of convergence could allow a large seal resistance R_{L} and small membrane capacitance C_{m} to be obtained while keeping R_{s} low. Thus the flexibility of geometry afforded by planar electrode designs should allow the first and third terms of (Eq. 17.4) to be kept small. The second term, the amplifier current noise, is basically the shot noise in the input transistor's leakage current. Small MOS transistors can have sufficiently small leakage currents, in the femtoampere range.

The big challenge is the last term, involving the capacitance and the amplifier voltage noise. Given an electrode with greatly reduced capacitance C_{e}, it should be matched with smaller amplifier capacitances. An order of magnitude reduction in all the capacitances seems possible. A decrease in amplifier voltage noise is also required, perhaps obtainable with very short channel field-effect transistors. Then if other noise sources not modeled here are also kept under control—dielectric noise being one of the most serious (Levis and Rae, 1998)—it may be possible to meet the grand challenge of detecting the movements of a few elementary charges.

The ability to detect such small charge movements would be of great interest in working out the mechanisms of ion pumps and co-transporters. These are proteins which transport ions individually or in small groups, where a conformational change, and sometimes the expenditure of metabolic energy, accompanies each ion movement. Small charge movements are also involved in the "gating charges" of voltage-gated ion channels. To observe these charge movements would illuminate the detailed kinetics of the voltage-transduction mechanism.

17.6 Future Prospects

Chip-based, planar patch-clamp instruments are already in use in the pharmaceutical industry for screening of compounds targeted to ion channels. There is still much to be done to improve this technology: the throughput of measurements is still one or two orders of magnitude below what is needed to do primary "high-throughput" screening of drug compounds. Increased levels of integration, involving multiple electrodes per chip and integrated microfluidics, will allow an increase in the number measurements

made in parallel. Integration of the electronics will also help: monolithic patch-clamp amplifiers and arrays, at least for whole-cell recording, should be possible to make.

Small chip-based instruments are becoming available also for research laboratories, where many large and expensive patch-clamp rigs will eventually be replaced by these benchtop instruments. In addition to the more routine measurements in ion-channel research, there are great benefits to be gained through the design of special microfabricated devices. One benefit is the possibility of rapid solution exchange on both sides of the partition, thanks to the integration of microfluidics. Another will be the possibility of single-molecule experiments in which both ionic current and fluorescence measurements are made from the same ion channel protein. New microfabricated devices will also make possible measurements of smaller currents thanks to reductions in capacitance that come from miniaturization.

Acknowledgment

This work was supported by National Institutes of Health Grant number EB004020.

References

Asmild, M., N. Oswald, K.M. Krzywkowski, S. Friis, R.B. Jacobsen, D. Reuter, R. Taboryski, J. Kutchinsky, R.K. Vestergaard, R.L. Schroder, C.B. Sorensen, M. Bech, M.P.G. Korsgaard, and N.J. Willumsen. 2003. Upscaling and automation of electrophysiology: Toward high throughput screening in ion channel drug discovery. *Receptors Channels* 9(1):49–58.

Baylor, S.M. 2005. Calcium sparks in skeletal muscle fibers. *Cell Calcium* 37(6):513–530.

Bezanilla, F. 2002. Voltage sensor movements. *J. Gen. Physiol.* 120(4):465–473.

Borisenko, V., T. Lougheed, J. Hesse, E. Fureder-Kitzmuller, N. Fertig, J.C. Behrends, G.A. Woolley, and G.J. Schutz. 2003. Simultaneous optical and electrical recording of single gramicidin channels. *Biophys. J.* 84(1):612–622.

Braun, D., and P. Fromherz. 2004. Imaging neuronal seal resistance on silicon chip using fluorescent voltage-sensitive dye. *Biophys. J.* 87(2):1351–1359.

Brown, A.M. 2004. Drugs, hERG and sudden death. *Cell Calcium* 35(6):543–547.

Cheng, H., W.J. Lederer, and M.B. Cannell. 1993. Calcium sparks—Elementary events underlying excitation–contraction coupling in heart-muscle. *Science* 262(5134):740–744.

Colquhoun, D., and F.J. Sigworth. 1995. Fitting and statistical analysis of single-channel records. *In*: Single-Channel Recording, 2nd Ed. B. Sakmann and E. Neher, editors. Plenum, New York. 483–587.

Demuro, A., and I. Parker. 2005. "Optical patch-clamping": Single-channel recording by imaging Ca^{2+} flux through individual muscle acetylcholine receptor channels. *J. Gen. Physiol.* 126(3):179–192.

Fertig, N., R.H. Blick, and J.C. Behrends. 2002. Microstructered glass chip for ion-channel electrophysiology. *Biophys. J.* 82(1):161A–161A.

Fertig, N., M. George, M. Klau, C. Meyer, A. Tilke, C. Sobotta, R.H. Blick, and J.C. Behrends. 2003. Microstructured apertures in planar glass substrates for ion channel research. *Receptors Channels* 9(1):29–40.

Fertig, N., A. Tilke, R. Blick, and J. Behrends. 2000. Nanostructured suspended aperture for patch clamp recording and scanning probe application on native membranes. *Biophys. J.* 78(1):266A–266A.

Fromherz, P. 2002. Electrical interfacing of nerve cells and semiconductor chips. *Chemphyschem* 3(3):276–284.

Gonzalez, J.E., and R.Y. Tsien. 1997. Improved indicators of cell membrane potential that use fluorescence resonance energy transfer. *Chem. Biol.* 4(4):269–277.

Guia, A., Y.B. Wang, J.Q. Xu, K. Sithiphong, Z.H. Yang, C.L. Cui, L. Wu, E. Han, and J. Xu. 2002. Micro-positioning enabled patch clamp recordings on a chip. *Biophys. J.* 82(1):161A–161A.

Hamill, O.P., A. Marty, E. Neher, B. Sakmann, and F.J. Sigworth. 1981. Improved patch-clamp techniques for high-resolution current recording from cells and cell-free membrane patches. *Pflugers Arch.* 391(2):85–100.

Handran, S., J. Constantin, A. Wittel, N. Yang, F. Livingston, D. Yamane, and A. Finkel. 2005. Population patch clamp technology: The second revolution in ion channel discovery. *In*: PharmaDiscovery. Washington, DC.

Hodgkin, A.L., A.F. Huxley, and B. Katz. 1952. Measurement of current–voltage relations in the membrane of the giant axon of loligo. *J. Physiol. Lond.* 116(4):424–448.

Hutzler, M., and P. Fromherz. 2004. Silicon chip with capacitors and transistors for interfacing organotypic brain slice of rat hippocampus. *Eur. J. Neurosci.* 19(8):2231–2238.

Ingebrandt, S., C.K. Yeung, M. Krause, and A. Offenhausser. 2005. Neuron-transistor coupling: Interpretation of individual extracellular recorded signals. *Eur. Biophys. J. Biophys. Lett.* 34(2):144–154.

Ionescu-Zanetti, C., R.M. Shaw, J.G. Seo, Y.N. Jan, L.Y. Jan, and L.P. Lee. 2005. Mammalian electrophysiology on a microfluidic platform. *Proc. Natl. Acad. Sci. USA* 102(26):9112–9117.

Kass, R.S. 2005. The channelopathies: Novel insights into molecular and genet mechanisms of human disease. *J. Clin. Invest.* 115(8):1986–1989.

Kiss, L., P.B. Bennett, V.N. Uebele, K.S. Koblan, S.A. Kane, B. Neagle, and K. Schroeder. 2003. High throughput ion-channel pharmacology: Planar-array-based voltage clamp. *Assay Drug Dev. Technol.* 1(1):127–135.

Klemic, K.G., J.F. Klemic, M.A. Reed, and F.J. Sigworth. 2002. Micromolded PDMS planar electrode allows patch clamp electrical recordings from cells. *Biosens. Bioelectron.* 17(6/7):597–604.

Author: Please check the page range.

Author: Please check the page range.

Author: Please check the page range.

Author: Please provide the name of the publisher.

Klemic, K.G., J.F. Klemic, and F.J. Sigworth. 2005. An air-molding technique for fabricating PDMS planar patch-clamp electrodes. *Pflugers Arch.* 449(6):564–572.

Lehnert, T., M.A.M. Gijs, R. Netzer, and U. Bischoff. 2002. Realization of hollow SiO_2 micronozzles for electrical measurements on living cells. *Appl. Phys. Lett.* 81(26):5063–5065.

Levis, R.A., and J.L. Rae. 1998. Low-noise patch-clamp techniques. *Methods Enzymol.* 293:218–266.

Neher, E., and B. Sakmann. 1976. Single-channel currents recorded from membrane of denervated frog muscle fibres. *Nature* 260(5554):799–802.

Neher, E., B. Sakmann, and J.H. Steinbach. 1978. The extracellular patch clamp: A method for resolving currents through individual open channels in biological membranes. *Pflugers Arch.* 375(2):219–228.

Pantoja, R., J.M. Nagarah, D.M. Starace, N.A. Melosh, R. Blunck, F. Bezanilla, and J.R. Heath. 2004. Silicon chip-based patch-clamp electrodes integrated with PDMS microfluidics. *Biosens. Bioelectron.* 20(3):509–517.

Rae, J., K. Cooper, P. Gates, and M. Watsky. 1991. Low access resistance perforated patch recordings using amphotericin-B. *J. Neurosci. Methods* 37(1):15–26.

Roden, D.M. 2004. Drug-induced prolongation of the QT interval. *N. Engl. J. Med.* 350(10):1013–1022.

Schmidt, C., M. Mayer, and H. Vogel. 2000. A chip-based biosensor for the functional analysis of single ion channels. *Angew. Chem. Int. Ed.* 39(17):3137–3140.

Sia, S.K., and G.M. Whitesides. 2003. Microfluidic devices fabricated in poly(dimethylsiloxane) for biological studies. *Electrophoresis* 24(21):3563–3576.

Sigworth, F.J. 1995. Electronic design of the patch clamp. *In*: Single-Channel Recording, 2nd Ed. B. Sakmann and E. Neher, editors. Plenum, New York, pp. 95–127.

Sonnleitner, A., L.M. Mannuzzu, S. Terakawa, and E.Y. Isacoff. 2002. Structural rearrangements in single ion channels detected optically in living cells. *Proc. Natl. Acad. Sci. USA* 99(20):12759–12764.

Stett, A., C. Burkhardt, U. Weber, P. van Stiphout, and T. Knott. 2003. Cytocentering: A novel technique enabling automated cell-by-cell patch clamping with the CytoPatch (TM) chip. *Receptors Channels* 9(1):59–66.

Terstappen, G. 1999. Functional analysis of native and recombinant ion channels using a high-capacity nonradioactive rubidium efflux assay. *Anal. Biochem.* 272:149–155.

van Stiphout, P., T. Knott, T. Danker, and A. Stett. 2005. 3D Microfluidic chip for automated patch-clamping. *In*: VDE Mikrosystemtechnik-Kongress. Technik VVdEEIeVaVVI, (VDI/VDE-IT) G, editors. Freiburg, Germany, pp. 435–438.

Vennekamp, J., H. Wulff, C. Beeton, P.A. Calabresi, S. Grissmer, W. Hansel, and K.G. Chandy. 2004. Kv1.3-blocking 5-phenylalkoxypsoralens: A new class of immunomodulators. *Mol. Pharmacol.* 65(6):1364–1374.

Author: Please check the names of editors.

Xu, J., A. Guia, D. Rothwarf, M.X. Huang, K. Sithiphong, J. Ouang, G.L. Tao, X.B. Wang, and L. Wu. 2003. A benchmark study with SealChip (TM) planar patch-clamp technology. *Assay Drug Dev. Technol.* 1(5):675–684.

Zeng, J.L., K.R. Laurita, D.S. Rosenbaum, and Y. Rudy. 1995. 2 Components of the delayed rectifier K^+ current in ventricular myocytes of the guinea-pig type—theoretical formulation and their role in repolarization. *Circ. Res.* 77(1):140–152.